

2020

β -Methylumbelliferone Surface Modification and Permeability Investigations at PENTEL™ Graphite Electrodes

Susan Warren

Brian Seddon

Ruth Pilkington

See next page for additional authors

Follow this and additional works at: <https://arrow.tudublin.ie/cenresart>

 Part of the [Chemistry Commons](#)

This Article is brought to you for free and open access by the Crest: Centre for Research in Engineering Surface Technology at ARROW@TU Dublin. It has been accepted for inclusion in Articles by an authorized administrator of ARROW@TU Dublin. For more information, please contact arrow.admin@tudublin.ie, aisling.coyne@tudublin.ie, gerard.connolly@tudublin.ie.



This work is licensed under a [Creative Commons Attribution-Noncommercial-Share Alike 4.0 License](#)
Funder: Higher Education Authority

Authors

Susan Warren, Brian Seddon, Ruth Pilkington, Alison Crossely, Philip Holdway, and Eithne Dempsey

β -Methylumbelliferone Surface Modification and Permeability Investigations at PENTEL™ Graphite Electrodes

Susan Warren,^{*,[a, b]} Brian Seddon,^[c] Ruth Pilkington,^[d] Alison Crossely,^[e] Philip Holdway,^[e] and Eithne Dempsey^[f]

Abstract: Electrochemical and micro-imaging analysis of a commercial graphite-composite material is presented following electro-oxidation with β -methylumbelliferone. Charge-transfer surface modification was observed for the graphite electrode, presumed to have arisen from adsorbed interfacial umbelliferone moieties. The molecular permeability of the new surface towards a range of

similar, yet size-variable (23 \AA^3 – 136 \AA^3) molecular redox probes is discussed. Red-shift fluorescence in confocal microscopy offers further support for the presence of a surface-bound umbelliferone layer. An SEM-platinum profiling technique was used as an imaging tool to map the umbelliferone surface and size-distribution of electro-active sites.

Keywords: β -methyl-umbelliferone · graphite pencil electrode · selective polymer layer

1 Introduction


The utility of graphite-composite pencil materials as electronic conductors and base electrodes has been recognised for many years with most of the early characterisation and development work having been conducted in Japan [1]. Pencil-graphite electrodes have proven to be robust electronic materials for molecular detection in single and multiple measurement experiments [2]. Screen printed graphite electrodes (SPCE) could be considered as an alternative to pencil graphite electrodes. However, SPCEs are single use only electrodes with a higher overall cost which make pencil graphite electrodes a more favourable option in some cases [3].

Graphite composites are finding applications in many different electro-analysis techniques and chemical sensors; notably protein and heavy-metal stripping analysis [4–5], and detectors for pharmaceuticals, such as acetylsalicylic acid [6], acetaminophen [7] and trepibutone [8]. Research in our laboratory has explored PENTEL™ graphite materials as charge transfer transducers and as immobilisation platforms for enzymes and antibody biomolecules. The material has been successfully employed in several immunoelectrode systems as well as methods in electrochemical iodimetry and oximetry [9].

The engineering of molecular surfaces by *in situ* electro-synthesis is being pursued for electrode-based devices in emerging micro-chemical instrumentation and remote biosensors. The drive behind molecular modifications of electrode surfaces include: (i) enhanced electro-catalysis, (ii) limitation of electrode fouling processes and (iii) prevention of undesirable reactions competing kinetically with the desired electrode process [10–11]. Commercial interest in electrodeposited polymer surfaces has led to the development of several clinical microelectrode

probes and biosensors, notably nitric oxide, catecholamine, acetylcholine. Introduction of such surface modification has brought about improvements in measurement selectivity based on size-charge membrane properties and has prolonged device utility by limiting fouling in complex media. Research in this area has been directed at electrochemically deposited films based on phenolic and aromatic amine monomers, some of which have not always displayed ideal membrane characteristics.

-
- [a] S. Warren
Centre for Research in Electroanalytical Techniques (CREATE), Centre of Applied Science for Health (CASH), Technological University Dublin – Tallaght Campus, Tallaght, Dublin 24, Ireland
Tel.: +353 (0)1 4027949
E-mail: susan.warren@TUDublin.ie
- [b] S. Warren
CREST Technology Gateway, Technical University Dublin – City Campus, Kevin St., Dublin 8, Ireland
- [c] B. Seddon
Microsensors for Clinical Research and Analysis (MiCRA Biodiagnostics), Centre of Applied Science for Health (CASH), Technological University Dublin – Tallaght Campus, Dublin 24, Ireland
- [d] R. Pilkington
Centre of Microbial Host Interactions (CMHI), Technological University Dublin – Tallaght Campus, Dublin 24, Ireland
- [e] A. Crossely, P. Holdway
Department of Materials, Oxford University, Oxford, Oxfordshire, United Kingdom
- [f] E. Dempsey
Department of Chemistry, Maynooth University, Maynooth, Ireland

 Supporting information for this article is available on the WWW under <https://doi.org/10.1002/elan.201900184>

Physical and electro-organic chemists have identified several families of organic molecules which can electrodeposit, forming either mono-molecular layers, or thick films. In both cases perturbation of electron-transfer behaviour for small redox molecules is observed. The umbelliferones, (coumarins) are one such class whose redox-electrode properties and electrochemistry have been largely overlooked. Umbelliferones are phytochemicals, comprising over 1300 natural derivatives [12,13]. These molecules are of biotechnological interest owing to their broad biological activities, efficacies spanning disease prevention, growth and antioxidant metabolics [14]. Their physico-chemical functionality has led to developments in chemo and opto-electronics research.

β -methylumbelliferone (7-hydroxy-4-methylcoumarin) is a coumarin analogue which has seen extensive clinical use. β -methylumbelliferone has a well characterised fluorescence whose intensity is pH-dependent [15] (λ_{max} pH 10). In contrast, esters of β -methylumbelliferone do not fluoresce unless cleaved to release the fluorophore. The change in electronic state has seen many β -methylumbelliferone derivatives exploited in a variety of enzyme-linked fluorometric assays, including β -galactosidase for liver activity [16], lipase activity characterisation from microbial origin [17], and β -glucuronidase for detection and enumeration of *E. coli* in water [18]. Scopletin, an umbelliferone derivative (7-hydroxy-6-methoxy-coumarin) has been attached to a gold electrode, utilising the molecular structure as a linkage surface for nucleic acid fragments and protein molecules [19]. Umbelliferone functionalised surfaces were found to be hydrophilic and easily wettable, suggesting the promotion of polar bonds during electrode deposition. The umbelliferone molecule adsorbs equally well on carbon surfaces with similar effect. X.-R. Hu *et al.* investigated the spectro-electrochemical characteristics of two representative umbelliferones: 7-hydroxycoumarin and 4-hydroxycoumarin concluding that electro-oxidation of both molecules leads to the formation of a non-conductive film on the electrode surface [20].

Our interest in electrochemical surface modification for improved analytical selectivity has led to studies of new organic interfaces on graphite-composite electrode materials. We have assessed one such umbelliferone modification for a commercial graphite material with known, “well-behaved” electrochemical characteristics in order to design functional chemical sensors with improved selectivity. This work focuses on the apparent improvement in charge-transfer selectivity for a series of redox probes at β -methylumbelliferone-graphite electrodes. An adherent, non-conductive umbelliferone layer with nanoscale pores is thought to contribute to the observed redox electrochemistry. Molecular fluorescence measurements, electron microscopy imaging and x-ray photoelectron spectroscopy were used to characterise the novel electro-synthesised surfaces.

2 Results and Discussion

2.1 Electrochemistry

2.1.1 β -Methylumbelliferone Film Formation

Cyclic voltammetry in Figure 1 represents the electrochemical behaviour of β -methylumbelliferone at a PENTEL graphite-composite electrode in carbonate electrolyte. The voltammetry indicates a single, oxidation process with a current maximum at ~ 0.7 V vs. Ag/AgCl. No reverse scan features were observed differentiating it from the background electrolyte, i.e. the umbelliferone molecule appears not to give rise to any observable reduction electrochemistry. Multiple-scan experiments, where the graphite electrode was used consecutively to oxidise β -methylumbelliferone, revealed changes in this voltammetric profile – peak currents diminish rapidly and the I - E characteristic changes from a diffusion-limiting electrode reaction to one that was kinetically impeded. It appeared that during the potential cycling, the electrode reaction of β -methylumbelliferone in carbonate electrolyte, progressively passivated the electrode surface to further oxidation of the β -methylumbelliferone molecule. This is a result commonly found with electrode fouling, surface deposition of reactive products and insulating-film formation. The rate of this apparent surface blocking was concentration dependent. It was observed that higher concentrations of umbelliferone induced a rapid deactivation response compared to lower concentrations. This supports the idea that even at the lower umbelliferone concentration, changes to the electrode surface occurred albeit more slowly. This may allow for better control of the surface modification or film-forming process. It has been observed that over time (cycle number 10–125), at all concentration levels (50 μM –2.5 mM), the degree of this deactivation approached a limiting value. Currents did not tend completely towards the background electrolyte, in fact a small degree of surface reactivity remained and complete coverage of the electrode did not occur. These observations suggested that it was unlikely that this was a multilayer deposition, a common feature of self-limiting insulating film formation.

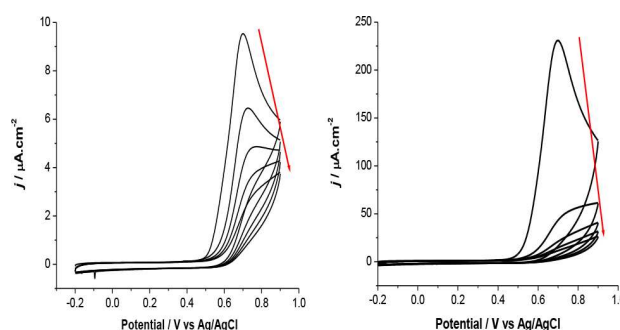


Fig. 1. Cyclic voltammograms of a) 250 μM and b) 1 mM βmU at PENTAL graphite electrodes in carbonate buffer at 0.1 V s^{-1} .

Further observations support the formation of a surface layer composed of an electronically insulating film. No distinguishable electrochemistry was observed for the β -methylumbelliferone molecule after the electrode was washed and returned to carbonate or phosphate buffer. Following β -methylumbelliferone electrodeposition, there was a noticeable change in the hydrophilic state of the carbon surface with an improvement in electrode wettability in comparison to the untreated graphite material, the latter displaying considerable hydrophobicity (see supporting information SI1). This phenomena has been observed and reported for similar hydroxy coumarin materials [19,21], being attributed to the formation of C–O bonds.

Voltammetric measurements with the umbelliferone-modified electrode revealed the degree of stability of the new surface. Aggressive anodic treatments, i.e. applying electrode potentials repeatedly beyond +1.0 V in basic electrolyte, re-instated the electro-activity of the graphite electrode to a condition observed prior to treatment, see supporting information (SI 2).

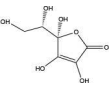
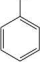
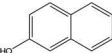
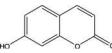
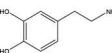
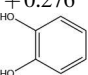
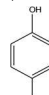
Glassy carbon and platinum electrodes were also modified with β -methylumbelliferone. Film formation was comparable on all 3 electrode types and exhibited comparable behaviour as described in the text.

2.1.2 Redox Molecule Interrogation at Modified Surface

The response of the β -methylumbelliferone electrode to redox species of different molecular structure was investigated by cyclic voltammetry. β -methylumbelliferone treatment altered the electron transfer characteristics of redox molecules at the electrode surface. Interest here focused on the relationship between probe molecular structure and observable electrode currents. A selectivity factor expressed as a “degree of hindrance”/ d_H , calculated from the ratio of current densities for the modified electrode and graphite-composite electrode. For example, the sampled current (e.g. peak current) for a redox process at the graphite electrode (electrolyte background subtracted) is, ΔI_g . Similarly, the current at the umbelliferone film electrode is given by, ΔI_{Umb} . Ratio, $\Delta I_{Umb}/\Delta I_g$ expresses the accessibility of a redox molecule to the umbelliferone film electrode surface. Hence, $1-\Delta I_{Umb}/\Delta I_g$ expressed as a percentage provides the degree of hindrance d_H the umbelliferone electrode offers to the underlying graphite electrode surface (Table 1). The peak current of the modified electrode was recorded at the peak voltage, irrespective of peak shift from the peak potential at the bare electrode. If no peak was present, the current was sampled at the peak potential obtained from the bare electrode.

The hexacyanoferrate (III) anion displayed hindered redox activity at the β -methylumbelliferone electrode, relative to the unmodified electrode (see supporting information SI 4) indicating some electrostatic repulsion at the modified electrode. A scan rate study revealed that the impeded redox response was diffusion controlled (SI 5) and

Table 1. Molecular parameters and hindrance values for 100 μ M electrochemical probes in PBS pH 7.4, analysed by cyclic voltammetry at 0.1 V s⁻¹;

Probe [pKa]	E_{OX}/V vs. Ag/AgCl	Volume/ \AA^3	d_H 250 μ M β mU ^a	d_H 1 mM β mU ^a
Ascorbic Acid [4.1, 11.6]	 + 0.699	139.7	85.8 KH	95.3 KH
Phenol [9.98] ²²	 + 0.709	92.1	82.6 KH	91.2 KH
2-Naphthol [9.5]	 + 0.566	136.1	76.8 KH	82.2 KH
Umbelliferone [7.11]	 + 0.741	136.6	77.5 KH	81.5 KH
Dopamine [8.5]	 + 0.276	145	40 DH	66 DH
Catechol [9.85]	 + 0.395	100.1	24.1 DH	44.2 DH
Hydroquinone [9.96]	 + 0.327	100.1	21.3 DH	54 DH

* Volume values calculated using *Molinspiration*²¹; ^a Concentration used for electrode modification process. KH – Kinetic Hindrance; DH – Diffusive Hindrance.

no increase in currents were evident upon repeated cycling. The cationic redox probe $\text{Ru}(\text{NH}_3)_6\text{Cl}_2$ resulted in a diffusion controlled response with electron transfer maintained at the modified graphite surface, indicating ease of access of the cationic species through the β -methylumbelliferone film with a reduction in anodic current and slight increase in ΔE_p (supporting information SI 6).

The electrochemistry of other redox molecules was restricted to some extent at the β -methylumbelliferone electrode compared to graphite alone. A list of redox molecules studied and their structural and electrochemical data is given in Table 1 below. The identification of molecular structural characteristics significant with respect to optimum electro-activity was investigated.

Of the molecules investigated, two distinct types of hindrance were observed – *kinetic* hindrance – whereby no distinctive redox peak was defined, as would be observed at a bare electrode; and *diffusive* hindrance where the redox peak was observed but shifted to higher potentials. Figure 2 a) and b) displays the cyclic voltammetry measurements for solutions of phenol and hydroquinone, highlighting the oxidation processes at both graphite and β -methylumbelliferone electrodes. Cyclic

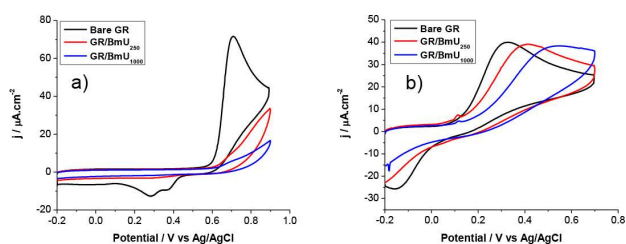


Fig. 2. Cyclic voltammograms (PBS pH 7.4, scan rate 0.1 V s^{-1}) indicating the d_H at the β -methylumbelliferone modified electrodes formed from 250 μM and 1 mM solutions for **a)** 100 μM phenol and **b)** 100 μM hydroquinone.

voltammetry of the other electrochemical probes can be found in supporting information (SI 7–11).

If β -methylumbelliferone surface modification resulted in behaviour solely as an inert, size-selective film it would be expected that the hindrance effect would increase with the molecular volume of the electrochemical probe. However, as evident from Table 1 a simple charge-transfer-molecule size trend was found to be the case [22] but with exceptions. Phenol is the smallest of the redox molecules examined in this set, yet it appears to show one of the highest hindrance indices of the probes investigated. The electrochemical probe studies show that all the mono-phenolic compounds in this study exhibit kinetic hindrance while the di-phenol species exhibited diffusive hindrance. These results may be explained in terms of the surface behaviour of the oxidising species.

The oxidation potential of phenol is observed to be very sensitive to pH and is concentration dependent – *i. e.* oxidation potential decreases with phenol concentration [23]. It has also been reported [24] that the anionic species of phenol is the most sensitive form to oxidation, while in the case of diphenols the rate of oxidation exhibits an apparent second-order dependency on the hydroxide ion concentration. Phenol and phenolic species are commonly known to cause fouling of electrode surfaces. This process is well documented [25–26] and tends to proceed via the formation of the phenoxy radical which can then react further with other phenol molecules to form a dimer radical. Oxidation of the dimer radical can occur by one of two pathways depending on the conditions used – high phenol concentration and basic pH favours polymerisation while low phenol concentration and acidic pH promotes quinone formation. Conditions applied in these experiments would support the polymerisation of the phenolic dimer radical, and this suggests that the selectivity of the film is based on blocking of further surface reactions occurring. For example, if we compare the cyclic voltammograms of the monophenolic redox probes at the β -methylumbelliferone modified electrode, with the final cycle of the β -methylumbelliferone formation, they exhibit a similar kinetic hindrance effect. The assumption is that under the conditions applied, all the monophenolic species in this study oxidise at the electrode surface, and further react to form an insoluble

surface layer. If the electrode surface is already coated with an insulating film this would prevent such a surface reaction and subsequent coating from occurring.

Hydroquinone, in contrast to phenol, has a relatively stable quinone form, shown as the less pronounced reduction peak $\sim -0.175 \text{ V vs Ag/AgCl}$. This electrochemical behaviour is also observed with catechol [27] and dopamine. d_H values for catechol and hydroquinone show that the β -methylumbelliferone film barely differentiates the two diphenolic molecules. The charge-transfer characteristic observed for phenol in comparison with the dihydroxybenzenes could be linked to phenol's electro-reactivity dependence on the anion form, the electrode reaction generating phenoxy radicals compared to more stable quinone.

The electrochemistry of 2-naphthol, another monophenol, strongly reflects the behaviour of phenol. However, we see that even though phenol was repelled from the β -methylumbelliferone electrode surface, 2-naphthol was only partially affected. Taking pK_a values into account, both molecules would be in their neutral form – 2-naphthol having similar yet more reactive nature than phenol (more stable radical formed). Umbelliferone, similar in structure to β -methylumbelliferone, shows electrochemistry close to that observed during the latter stages of β -methylumbelliferone electrode modification. It is important to note that umbelliferone shows a defined redox peak at the modified electrode while β -methylumbelliferone does not (SI 9). Molecules bearing large hydration shells also displayed restricted charge transfer kinetics, notably ascorbic acid, being partially ionised at the pH employed.

2.1.3 SEM Imaging of β -Methylumbelliferone Surface and Platinum Profiling

SEM imaging studies of a fractured β -methylumbelliferone electrodeposited layer on platinum wire were conducted to determine the layer thickness, $\sim 550 \text{ nm}$, and surface morphology (Figure 3). In support of the redox molecule study above, where there is some remaining electroactivity after surface modification, the layer morphology is observed to consist of a degree of porosity.

To further affirm this perceived porosity, platinum profiling experiments were conducted to demonstrate the

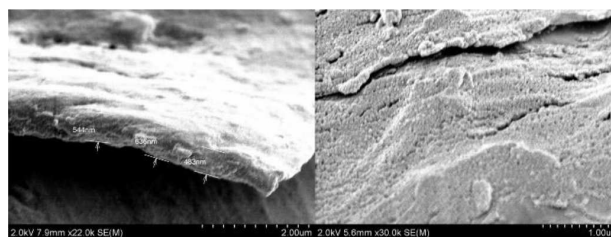


Fig. 3. SEM images of fractured β -methylumbelliferone modified platinum wire demonstrating layer porosity.

degree of electro-activity for the β -methylumbelliferone modified surface vs that of the bare graphite.

Platinum electro-deposition is a versatile technique to visualise the micro-electrochemical structure of charge-transfer surfaces. It is particularly useful in revealing surface distributions of electro-active sites in conductor-insulator composite materials. In our case, interest is focused on active-site densities on the graphite-composite electrode and the variations in distribution following β -methylumbelliferone deposition. In this set of experiments, platinum deposition was applied using two different potential ranges: (a) $+0.9 \rightarrow -0.25$ V vs Ag/AgCl and (b) $+1.2 \rightarrow -0.25$ V vs Ag/AgCl at $0.5 \text{ V}\cdot\text{s}^{-1}$; the number of cycles varied from 5–75.

Figure 4 is composed of a series of SEM images of the graphite-composite and β -methylumbelliferone modified electrodes showing the effects of platinum deposition ($+0.9 \rightarrow -0.25$ V vs Ag/AgCl at $0.5 \text{ V}\cdot\text{s}^{-1}$). As a general case for the graphite-composite electrode, it was observed that as the number of deposition cycles increased from 10 to 75, the Pt particles over the surface increased randomly in number and in size from *ca.* 100 to 300 nm). This contrasts with the β -methylumbelliferone electrodes where larger

structures (up to 800 nm) with greater inter particle distances were observed. A proposed mechanism for Pt electrodeposition is shown schematically in SI 12 whereby Pt initially deposits on an exposed area of the electrode, with further deposition occurring on the original site of deposition to form larger structures upon subsequent potential sweeping.

Figure 5 are images of the electrodes prepared using a higher anodic potential limit during platinum deposition ($+1.2 \rightarrow -0.25$ V vs Ag/AgCl at $0.5 \text{ V}\cdot\text{s}^{-1}$). Previous β -methylumbelliferone film studies showed that repeatedly applying voltages $> +1.0$ V vs Ag/AgCl, caused partial degradation of the film, finally resulting in complete electrode surface renewal. By subjecting the β -methylumbelliferone electrode to potentials $> +0.9$ V vs. Ag/AgCl we can effectively etch the film during the anodic sweep while depositing platinum on the cathodic sweep so that the film degradation process can be visualised.

The SEM images for these electrodes show quite different structures when compared to those in Figure 4. As before, the control electrodes exhibit an increase in particle number with increasing deposition time, but the Pt on the β -methylumbelliferone electrode surface grow from “crab” like to “kidney” like shapes. These structures reflect film degradation at $+1.2$ V vs. Ag/AgCl, as with each potential sweep more exposed surface area becomes

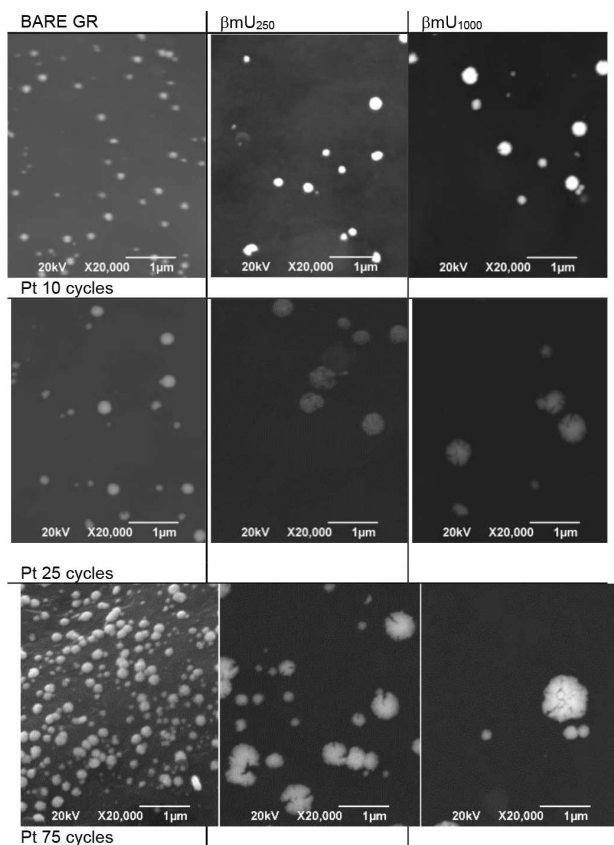


Fig. 4. SEM images of platinum profiling on control graphite electrodes and β -methyl umbelliferone modified electrodes formed from $250 \mu\text{M}$ and 1 mM β -methyl umbelliferone solutions. Platinum deposition was controlled by the number of potential cycles (10–75) applied during the deposition at $0.5 \text{ V}\cdot\text{s}^{-1}$ between $+0.9 \rightarrow -0.25 \text{ V}\cdot\text{s}^{-1}$.

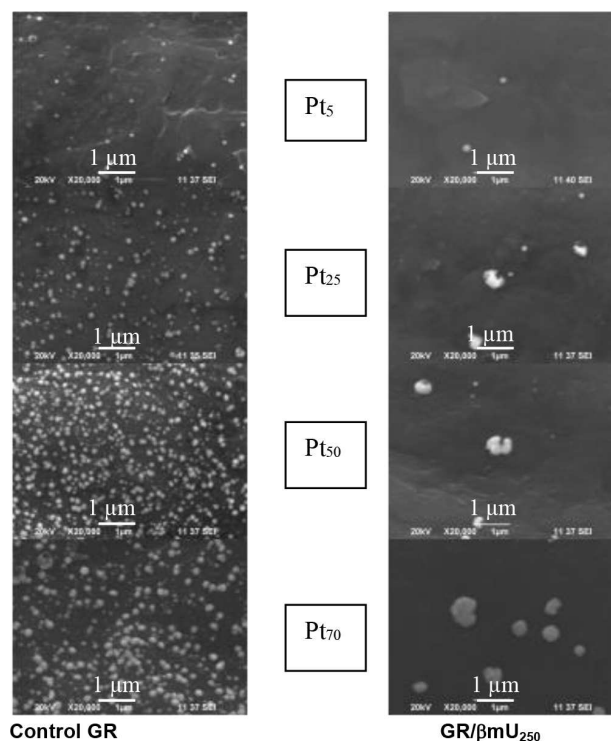


Fig. 5. SEM images of platinum profiling on control graphite electrodes (GR) and β -methyl umbelliferone GR modified electrodes formed from $250 \mu\text{M}$ β -methyl umbelliferone solution. Platinum deposition was controlled by the number of potential cycles applied during the deposition at $0.5 \text{ V}\cdot\text{s}^{-1}$ between $+1.2 \rightarrow -0.25 \text{ V}\cdot\text{s}^{-1}$.

available for deposition around the original site resulting in 'denser' structures.

Platinum profiling experiments demonstrated the degree of electro-activity for the base graphite material and allowed comparison after β -methylumbelliferone modification. β -methylumbelliferone oxidation certainly deactivates the electrode surface resulting in far fewer electro-active sites on which platinum nucleation can commence. This result is consistent with a partial filming process, leaving the surface a patchwork of insulating and charge-transfer regions. Platinum profiling experiments at the higher β -methylumbelliferone deposition potential result in the formation of different structures, as the film is etched slightly with each deposition sweep. The platinum structures formed in this case appear denser, reflecting a region at the interface between the particle edge and the anodically stripped region of the film. This contrasts with the individual zones of electroactivity evident in the presence of a more consistently intact film (Figure 5).

2.1.4 Solid-state Fluorescence

Owing to the fluorescent nature of β -methyl-umbelliferone, visualisation of the surface adsorbed molecules and films on carbon supports was tested using confocal microscopy techniques. Confocal images for β -methylumbelliferone treated carbon are shown in Figure 6. In aqueous solutions the β -methylumbelliferone molecule exhibits

fluorescence: at pH 10.2, excitation at 365 nm provides an emission signal at 445 nm. Thus for β -methylumbelliferone in solution a blue fluorescence was expected over a wide pH range [28].

Carbon materials exposed to aqueous solutions of β -methylumbelliferone were studied for solution-solid adsorption characteristics. Control experiments were also performed which consisted of carbon exposed to basic electrolyte. These controls displayed little or no fluorescence emission, while the carbon treated with β -methylumbelliferone solution showed an intense and uniform blue fluorescence. In electrochemical oxidation experiments of β -methylumbelliferone an interesting combination of blue and green fluorescence was observed; the latter being more prevalent.

Zhao *et al.* [29] investigated the solid and solution phase fluorescence of some poly(iptycenebutadiynylene) molecules, and showed that the solid spectra exhibited only a minor red shift (a few nm) in the emission maxima compared to the solution phase molecule. Brittain [30] studied the solid-state fluorescence of amoxicillin and ampicillin observing that these structurally similar molecules exhibited red shifts in their emission maxima of 8 nm and 48 nm respectively, from solution to solid spectra. For β -methylumbelliferone on carbon material, if the observed red shift (60 nm) was due solely to solid-state β -methyl-umbelliferone, then the carbon should show similar moderate red-shift fluorescence which it does not. The fluorescence imaging data suggests that a different electronic state of β -methylumbelliferone exists on the carbon surface. This significant red shift in the emission spectrum could be attributed to a local pH alkaline shift upon electrochemical oxidation during the formation of adsorbed β -methylumbelliferone dimers. The green fluorescence at 500 nm has also been attributed to the photolysis product 2,4-dihydroxy cinnamic acid which has been reported for substituted coumarins [27].

Electrochemical measurements show a passivation effect following deposition of β -methylumbelliferone. Surface passivation by electrode reaction products seems likely – umbelliferone radicals combining with active sites or dimerisation with a subsequent chemisorption process. The ease of surface renewal, *i.e.* occurring readily around +1 V vs Ag/AgCl, suggests breaking of weak $-C-O-C-$ bonds (according to the electrooxidative mechanism proposed below Scheme 1) rather than $-C-C-$ framework linkages. This electrochemical observation also discounts multi-layering and thick-film electro-polymerisation, since most such surfaces are irreversibly formed or require excessive electrolysis for the partial removal of surface films. The redox probe study confirmed that the remaining electro-active regions of the β -methylumbelliferone graphite electrodes are sensitive to certain types of molecular structure.

2.2.5 X-Ray Photoelectron Spectroscopy

XPS was done on a dropcast solution of β -methylumbelliferone on ITO and an electrodeposited layer of β -

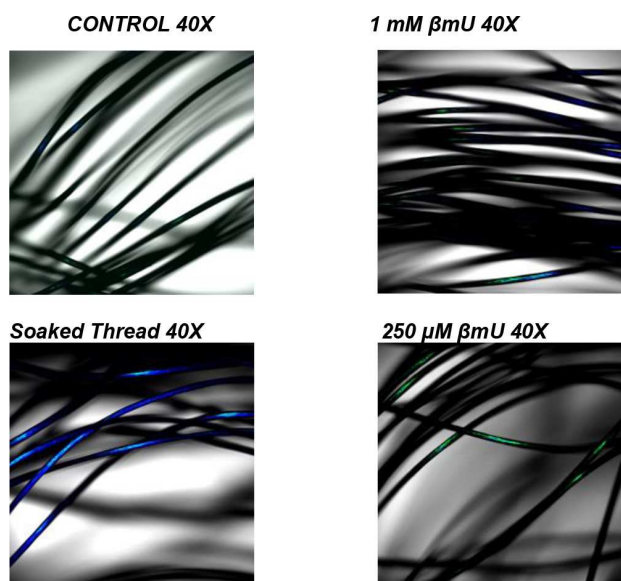
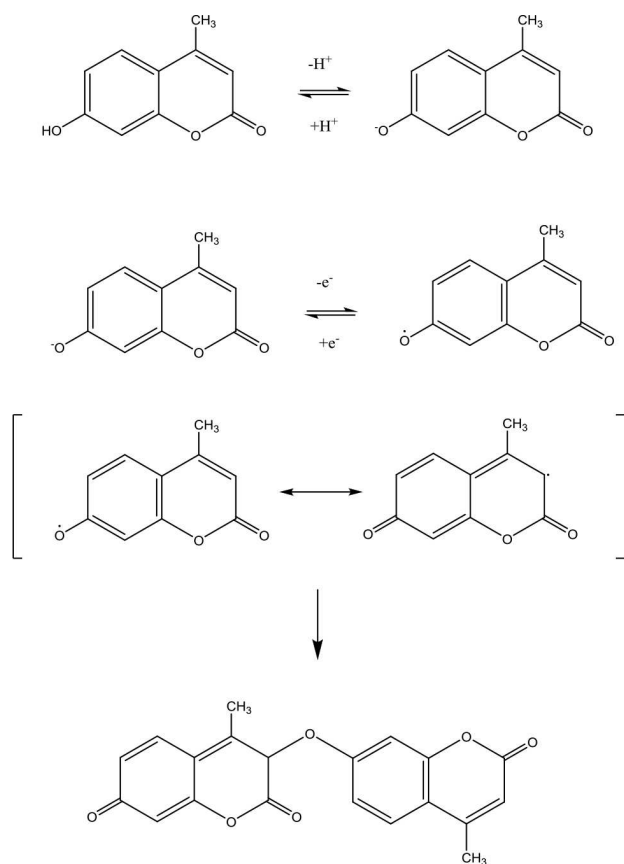


Fig. 6. Confocal images (40X) of carbon threads (approx. 500 μ m) modified with β -methyl umbelliferone. a) control carbon fibre untreated with β -methyl-umbelliferone, b) carbon fibre exposed to β -methylumbelliferone (1 mM) for 2 minutes then air dried, c) carbon fibre electrochemically modified β -methylumbelliferone (250 μ M) by the same procedure as the graphite rod. In the case of the electrochemically modified fibre, they were well rinsed with deionised water after modification and then dried. Each image contains the optical image, with the two laser configurations overlaid.



Scheme 1. Proposed electro-oxidative mechanism for β -methylumbelliferone based on [19].

methylumbelliferone on platinum wire. The C1s spectra overlay (see Supporting Information SI. 13) clearly shows an increase in $-C-O-C-$ bonds for the electrodeposited β -methylumbelliferone layer on platinum in comparison to a dried β -methylumbelliferone solution on ITO. This supports the proposed mechanism as described above and outlined in Scheme 1.

3 Conclusions

The question being considered by this work relates to the nature of the electrode surface following β -methylumbelliferone modification of graphite surfaces. Charge-transfer characteristics for a series of redox molecules are certainly altered with respect to electrochemical response observed. The selective characteristics of the new graphite- β -methylumbelliferone electrode are of interest and offer potential use in chemical analysis.

Electrochemical oxidation of β -methylumbelliferone in high pH carbonate electrolyte was observed at a graphite-composite electrode with surface passivation. The newly formed surface is partially electro-active, hydrophilic and stable in electrochemical experiments in cathodic and anodic regions ($< +0.9$ V vs. Ag/AgCl). The original surface can be regenerated by anodic electrolysis at electrode potentials $> +1.0$ V. The relative ease of

surface regeneration suggests the unlikely formation of an adherent umbelliferone polymer on the graphite.

SEM imaging of the β -methylumbelliferone layer shows that the surface morphology contains a degree of porosity. Platinum profiling experiments demonstrated the density and distribution of electro-active sites on the graphite, which is consistent with porous film formation. Electrochemistry with various redox molecules confirmed the β -methylumbelliferone treated electrode displays charge-transfer hindrance. The data leads to the conclusion that the new surface possesses properties consistent with some size-selective characteristics with bulky molecules, with large hydration volumes, displaying lower voltammetric currents than smaller redox molecules. Two exceptions to this trend are phenol and dopamine redox probes possibly due to possible blocking of surface reactions following phenolic dimer radical formation in the case of phenol and to the anionic nature of the latter. There also appeared to be a weak link between % hindrance (d_H) and increasing anodic oxidation potential (E_p) for the compounds studied.

Further support for the presence of surface umbelliferones came from confocal microscopy. The technique demonstrated red-shift fluorescence for carbon-adsorbed β -methylumbelliferone and provided spectral data for the existence of umbelliferone surface species following electro-oxidation.

Taking the electrochemical, imaging and other evidence on this electrode system into consideration, we conclude that the β -methylumbelliferone remains on the graphite surface as a non-conductive film. Such a surface may consist of single umbelliferone molecules bonded to the carbon frame, or an electro-adsorbed dimeric species formed during a radical-radical coupling. The β -methylumbelliferone electrode presented in this study has demonstrated some interesting charge-transfer characteristics for redox probes of similar molecules structure.

4 Experimental Section

4.1 Electrochemistry

Electrochemical measurements were performed on a CHI660c Electrochemical Workstation (CH Instruments, USA). For cyclic voltammetry and chronocoulometry studies a single-compartment electrochemical cell was used with a platinum counter electrode and Ag/AgCl | 3 M KCl reference for aqueous solutions. Working electrodes were commercially available PENTAL graphite composite rods, sealed with a polycarbonate lacquer to leave an exposed electrode tip of ~ 3 mm. All solutions were degassed for a minimum of 10 minutes prior to use with high purity Argon.

4.2 SEM Imaging

Electron microscopy (Hitachi SU-70) is used to characterise the fractured β -methylumbelliferone surface on a platinum wire to measure layer thickness and surface morphology. Electro-active site investigations were accomplished by platinum-profiling method. This involves controlled electro-deposition of platinum metal followed by SEM imaging (Joel LV-6390) of the particulate

metal distribution over the electrode surface. SEM analysis was also performed on vertical sections of graphite material. Section mounting was accomplished by epoxy-resin potting, cured with an amine-based cross-linking agent. Graphite specimens were polished to a smooth finish using relevant grades of alumina pads (Buehler) and washed with copious amounts of deionised water. The mount was sputter coated with Au/Pd (SC7620 Quorum Technologies) to minimize charging.

4.3 XPS Analysis

Samples were analysed using a Thermo Scientific K-Alpha XPS instrument equipped with a microfocussed monochromated Al X-ray source. The source was operated at 12 keV and a 400 micron spot size was used. The analyser operates at a constant analyser energy (CAE) 200 eV for survey scans and 50 eV for detailed scans.

Charge neutralization was applied using a combined low energy/ion flood source. The data acquisition and analysis was performed with Thermo Scientific Avantage software.

4.4 Confocal Microscopy

Fluorescence measurements were carried out with a confocal microscope (Olympus FV1000) using a 40x oil objective. The opaque nature of the graphite-composite material hindered attempts to analyse transmitted light, thus preventing detection of the β -methylumbelliferone molecule on electrode surfaces. To overcome this complication, carbon threads of micrometer-scale dimension were employed. These carbon threads were composed of a bundle of individual carbon fibers, each with a 10 μm diameter, resulting in an overall diameter of approximately 500 μm . The multi-fibrous nature of these materials allowed for light transmission and were suitable for confocal analysis of the interaction of β -methylumbelliferone with a carbon surface. The configuration of the experiment was such that for the excitation wavelength of 495 nm, an emission at 521 nm (green) was observed and an excitation signal at 358 nm, rendered a fluorescence emission maximum at 461 nm (blue). Prior to modification with β -methylumbelliferone, carbon threads were soaked in a 1:1 IPA/water mixture to ensure uniform wetting. Following β -methylumbelliferone modification the threads were rinsed with copious deionised water and allowed to air dry for 1–2 hours prior to confocal microscopy. Two controls were prepared, the first was a carbon thread without β -methylumbelliferone modification, and the second control was a carbon thread soaked in a 1 mM β -methylumbelliferone solution for 1 hour, which was allowed to air dry without rinsing.

4.5 Materials and Reagents

SEM potting epoxy-resin reagents were from Araldite. Graphite composite material was the extrusion pencil lead Hi-Polymer HB (PENTEL Pencil Co, Japan). Individual carbon fibres (~500 μm) from carbon cloth were from Clean Fuel Cell Energy, USA. ELGA LabWater provided deionised water with pH monitored consistently to ensure neutral pH. β -methylumbelliferone, β -naphthol, poly(propylenecarbonate), dopamine hydrochloride, sulphuric acid, potassium hexachloroplatinate (IV), potassium ferricyanide, tetrahydrofuran, were purchased from Sigma Aldrich and used as received unless otherwise specified. Phosphate buffered saline (PBS) pH 7.4 was a formulation of: NaCl (137 mM), KCl (2.7 mM), Na_2HPO_4 (10 mM), K_2HPO_4 (2 mM). Carbonate buffer, pH 9.6, consisted of sodium carbonate (30 mM) and sodium bicarbonate (70 mM). Premier grade Argon

(Air Products) was used for degassing all solutions. Electrolyte solutions of all molecular redox probes were made up as a stock solution of H_2SO_4 (0.1 M) prior to dilution (10 μl to 3 cm^3) with PBS solution. Owing to solubility issues both 2-naphthol and umbelliferone reagents were prepared in carbonate buffer solution at pH 9.6.

4.6 Procedures

4.6.1 Graphite- β -methylumbelliferone Electrode

Graphite- β -methylumbelliferone electrodes were fabricated from a base graphite composite material used in the manufacture of commercial fine pencil lead, 0.5 mm (HB Hi-Polymer, PENTEL Pencil Co). In this work, the graphite rod was partially coated with a polycarbonate film material by capillary insertion technique. This procedure allows control of a thick-film insulator over the graphite surface. Poly(propylenecarbonate), M_w 50,000, was dispersed in THF solvent (50 mg/ml) and 20 μl pipetted into a 0.75 mm diameter glass capillary. The graphite rod was inserted into the capillary, and then withdrawn. This rendered an insulating polymer coating of <10 μm thickness over the barrel of the graphite conductor. Polycarbonate films were formed by thermal treatment at 60 °C for 2 hrs. The rods retained an exposed tip section of approximately 3 mm. Insulation coatings, electrode area and surface structure were examined by SEM imaging which confirmed the integrity of the insulation layer, adherence to the graphite and film uniformity. Solvent deposited polycarbonate layers on graphite appeared as glassy films, durable and offering excellent electrical insulating characteristics. Electron microscopy images of graphite material show the extent of the base material's surface roughness, which may cause variation in active surface area.

Prior to surface treatments, graphite electrodes were examined by cyclic voltammetry, scanning electrode potential between 0 and +1.0 V vs. Ag/AgCl in 0.1 M PBS (pH 6) for 10 repeat cycles. This electro-oxidative voltammetry was necessary in order to assess the level of electrochemistry associated with the graphite-composite surface and to ensure a reproducible background current-potential (I - E) response. Cyclic voltammetry shows no inherent electrochemistry for the graphite electrode or polycarbonate film. Modification of the graphite electrode with β -methylumbelliferone was performed with freshly prepared solutions (0.25–2.5 mM) in carbonate buffering electrolyte, cycling from -0.2 V→0.9 V vs Ag/AgCl at 0.1 Vs^{-1} for 5 cycles. After surface modification, the electrode was well rinsed with deionised water, and cycled in PBS, from 0.0 V→0.9 V vs. Ag/AgCl at 0.1 Vs^{-1} for 16 cycles to ensure stable currents were achieved before analysis.

4.6.2 Electrode Size

The physical nature of the graphite electrode surface is not microscopically smooth, nor is the material a perfectly geometric cylinder. The graphite rod is actually a composite material – being a blended graphite material with a proprietary low temperature thermoplastic resin. The exposed electrode surface may therefore be considered a random orientation of graphite particles interspersed within an electronically insulating polymer. The extrusion manufacture of this composite gives rise to a circular section with a regular, undulated surface contour (peak-to-peak 20 μm). For these reasons, averaged diameter calculations based on imaging alone will provide a rough estimate of the true surface area of the electrode. The calculation can be refined and better estimate of “electrochemical area” achieved by an

electrolysis method. Active electrode area determination can be performed by a short-time chronocoulometry measurement. The technique applies the Anson equation [22]:

$$Q = \frac{2nFAC\sqrt{D}\sqrt{t}}{\sqrt{\pi}} + Q_{dl} + Q_{ads}$$

where n is the number of electrons, F is Faradays constant, C , concentration $[\text{Fe}(\text{CN})_6]^{3-}$, D , diffusion coefficient of $[\text{Fe}(\text{CN})_6]^{3-}$, t , time, Q_{dl} – charge associated with double layer, and Q_{ads} – charge associated with an adsorbed species [31]. Suitable potentials were chosen from an initial cyclic voltammogram, i.e. the potential was stepped from a region before reduction, i.e. +0.6 V, to a region where the current was diffusion controlled, typically about 0.0/–0.1 V, beyond the $E_{1/2}$ for the $\text{Fe}^{3+/2+}$. Short-time electrolysis (0.25 s) of potassium ferricyanide was followed at several concentrations (2.5, 5 and 10 mM) in 0.1 M KCl electrolyte. From an accurately known value of D ($0.76 \times 10^{-5} \text{ cm}^2 \text{ s}^{-1}$ [32]), it was possible to assess the electrochemically active area A of the electrode surface. Average electrochemical active electrode area was calculated as $0.0595 \pm 0.0098 \text{ cm}^2$ ($n = 5$). This value was found to be only 3.5 % greater than that calculated using area measurements taken with Vernier callipers ($0.0574 \pm 0.003 \text{ cm}^2$ where $n = 5$).

4.6.3 Electro-active Surface Investigations via Pt Deposition

Electro-deposition of platinum metal was studied in this work in order to aid visualisation of electro-active sites across the graphite material surface, before and after surface treatment with the umbelliferone reagent. The plating methodology and procedure were optimised in order to obtain the most consistent and uniform platinum deposition and size distribution so that any variations in the structure could be attributed to the presence of the β -methylumbelliferone film. The plating electrolyte consisted of K_2PtCl_6 (1 mM) in acid electrolyte (H_2SO_4 , 0.1 M) maintained under Argon at all times. Graphite electrodes were cycled over two different potential ranges; between (a) +0.9 → –0.25 V vs Ag/AgCl and (b) +1.2 → –0.25 V vs Ag/AgCl at $0.5 \text{ V}\cdot\text{s}^{-1}$; the number of cycles varied from 5–75 depending on the metal loading required. For each Pt electro-deposition on a β -methylumbelliferone electrode, the same procedure was followed for an untreated graphite electrode as a control. Following electroplating the graphite electrode was rinsed copiously with deionised water, returned to H_2SO_4 (0.5 M) electrolyte and cycled between the respective potential ranges as before, at $0.1\text{--}0.5 \text{ V}\cdot\text{s}^{-1}$ for 3 cycles in order to confirm successful Pt deposition.

Acknowledgements

The authors acknowledge the Programme for Research in Third Level Institutions Cycle 4, Higher Education Authority for the financial support to carry out this work.

References

- [1] H. Kaneko, A. Negishi, Y. Suda, *Electrochemical Society Proceedings* **1997**, 97, 433–439.
- [2] A. M. Bond, P. J. Mahon, J. Schiewe, V. Vincente-Beckett, *Anal. Chim. Acta* **1997**, 345, 67–74.
- [3] Md. R. Akanda, M. Sohail, Md. A. Aziz, A-N. Kawde, *Electroanalysis*, **2016**, 28, 408–424.
- [4] J. Wang, A. N. Kawde, E. Sahlin, *Analyst* **2000**, 125, 5–7.
- [5] M. J. Goldcamp, M. N. Underwood, J. L. Cloud, S. Harshman, *J. Chem. Educ.* **2008**, 85, 976–979.
- [6] V. Supalkova, J. Petrek, L. Havel, S. Krizkova, J. Petrlova, V. Adam, D. Potesil, P. Babula, M. Beklova, A. Horna, R. Kizek, *Sensors* **2006**, 6, 1483–1497.
- [7] P. Masawat, S. Liawruagrath, Y. Vaneesorn, B. Liawruagrath, *Talanta* **2002**, 58, 1221–1234.
- [8] W. Gao, J. Song, N. Wu, *J. Electroanal. Chem.* **2005**, 576, 1–7.
- [9] D. Rathod, S. Warren, B. Seddon, B. Singh and E. Dempsey, *Electroanalysis* **2015**, 27, 166–176.
- [10] S. J. Dong, G. L. Che, Y. W. Xie in *Chemically Modified Electrodes*. Chinese Science Press, Beijing, **1995**, pp. 39.
- [11] W. Ren, H. Q. Luo, N. B. Li, *Biosens. Bioelectron.* **2006**, 21, 1086–1092.
- [12] A. Lacy, R. O'Kennedy, *Curr. Pharm. Des.*, **2004**, 10, 3797.
- [13] A. Alemdar, A. R. Ozkaya, M. Bulut, *Polyhedron* **2009**, 28, 3788–3796.
- [14] J. Z. Pedersen, C. Oliverira, S. Incerpi, V. Kumar, A. M. Fiore, P. D. Vito, A. K. Prasad, S. V. Malhotra, V. S. Parmar, L. Saso, *J. Pharm. Pharmacol.* **2007**, 59, 1721–1728.
- [15] J. A. R. Mead, J. N. Smith, R. T. Williams, *Biochem. J.*, **1955**, 61, 569–574.
- [16] J. B. J. McGuire, T. J. James, C. J. Imber, S. D. St. Peter, P. J. Friend, R. P. Taylor, *Clin. Chim. Acta* **2002**, 326, 123–129.
- [17] N. Prim, M. Sanchez, C. Ruiz, F. I. J. Pastor, P. Diaz, *J. Mol. Catal. B* **2003**, 22, 339–346.
- [18] D. Wildeboer, L. Amirat, R. G. Price, R. A. Abuknesha, *Water Res.* **2010**, 44, 2621–2628.
- [19] N. Gajovic-Eichelmann, E. Ehrentreich-Forster, F. B. Bier, *Biosens. Bioelectron.* **2003**, 19, 417–422.
- [20] X.-R. Hu, J.-B. He, Y. Wang, Y.-W. Zhu, J.-J. Tian, *Electrochim. Acta* **2011**, 56, 2919–2925.
- [21] Q. Wu and H. D. Dewald, *Electroanalysis* **2001**, 13, 45–48.
- [22] <http://www.molinspiration.com>.
- [23] G. Arslan, B. Yazici, M. Erbil, *J. Hazard. Mater.* **2005**, B124, 37–43.
- [24] K. A. Connors, G. L. Amidon, V. J. Stella, in *Chemical Stability of Pharmaceuticals: a handbook for pharmacists 2nd Edition*, John Wiley and Sons Inc., **1986**, pp. 63–90.
- [25] G. Mengoli, S. Daolio, M. M. Musiani, *J. Appl. Electrochem.*, **1980**, 10, 459–471.
- [26] J. L. N. Xavier, E. Ortega, J. Z. Ferreira, A. M. Bernardes, V. Perez-Herranz, *Int. J. Electrochem. Sci.*, **2011**, 2, 622–636.
- [27] B. Nasr, B. Abdellatif, P. Canizares, C. Saez, J. Lobato, M. A. Rodrigo, *Environ. Sci. Technol.* **2005**, 39, 7234–7239.
- [28] D. W. Fink, W. R. Koehler, *Anal. Chem.* **1970**, 42, 990–993.
- [29] D. Zhao, T. M. Swager, *Macromolecules*, **2005**, 38, 9377–9384.
- [30] H. G. Brittain, *AAPS PharmSciTech*, **2005**, 6, E444–E448.
- [31] W. R. Heineman, P. T. Kissinger, in *Laboratory Techniques in Electroanalytical Chemistry* (Eds.: W. R. Heineman, P. T. Kissinger), Marcel Dekker, Inc. **1996**, 51–126.
- [32] A. J. Bard, L. R. Faulkner (Eds), *Electrochemical Methods, Fundamentals and Applications*, John Wiley & Sons Inc., **2001**, 813.

Received: March 18, 2019

Accepted: December 11, 2019

Published online on January 9, 2020